

Implementation of the SP3 equations in a MOOSE-based application

Roberto Fairhurst Agosta

NPRE 555
University of Illinois at Urbana-Champaign

December 16, 2020



Outline

① Introduction

Objectives

② Methodology

MOOSE

SP_3

Kernels

Diffusion solver

C5 MOX Benchmark

③ Results

1-D test case

2-D test case

④ Conclusions

Conclusions



Objectives

- Implement and solve SP_3 equations with a MOOSE-based application for the following cases:
- one-dimensional models:
 - fixed source problem with one energy group,
 - eigenvalue problem with one energy group,
 - fixed source problem with multiple energy groups,
 - eigenvalue source problem with multiple energy groups,
 - compare results to diffusion solver,
- two-dimensional model: C5 MOX Benchmark [3].

Outline

1 Introduction

Objectives

2 Methodology

MOOSE

SP_3

Kernels

Diffusion solver

C5 MOX Benchmark

3 Results

1-D test case

2-D test case

4 Conclusions

Conclusions

MOOSE



- Computational framework
- Solves coupled equation systems
- MOOSE defines weak forms
- MOOSE and LibMesh translate them into residual and Jacobian functions
- Petsc solution routines solve the equations

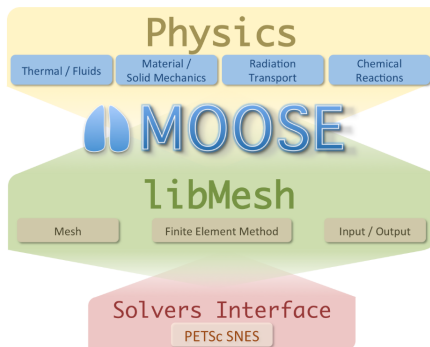


Figure: MOOSE framework. Image reproduced from [4].

P_3 equations

$$\frac{d}{dx}\phi_{1,g} + \Sigma_{t,g}\phi_{0,g} = \sum_{g'=1}^G \Sigma_{s0,g' \rightarrow g}\phi_{0,g'} + \frac{\chi_g}{k_{eff}} \sum_{g'=1}^G \nu \Sigma_{f,g'}\phi_{0,g'} + Q_{0,g} \quad (1)$$

$$\frac{1}{3} \frac{d}{dx}\phi_{0,g} + \frac{2}{3} \frac{d}{dx}\phi_{2,g} + \Sigma_{t,g}\phi_{1,g} = \sum_{g'=1}^G \Sigma_{s1,g' \rightarrow g}\phi_{1,g'} + Q_{1,g} \quad (2)$$

$$\frac{2}{5} \frac{d}{dx}\phi_{1,g} + \frac{3}{5} \frac{d}{dx}\phi_{3,g} + \Sigma_{t,g}\phi_{2,g} = \sum_{g'=1}^G \Sigma_{s2,g' \rightarrow g}\phi_{2,g'} + Q_{2,g} \quad (3)$$

$$\frac{3}{7} \frac{d}{dx}\phi_{2,g} + \Sigma_{t,g}\phi_{3,g} = \sum_{g'=1}^G \Sigma_{s3,g' \rightarrow g}\phi_{3,g'} + Q_{3,g}. \quad (4)$$

Assumptions [2]:

- isotropic external source
- negligible anisotropic group-to-group scattering

P_3 equations (2)

$$\frac{d}{dx}\phi_{1,g} + \Sigma_{0,g}\phi_{0,g} = \sum_{g' \neq g}^G \Sigma_{s0,g' \rightarrow g} \phi_{0,g'} + \frac{\chi_g}{k_{eff}} \sum_{g'=1}^G \nu \Sigma_{f,g'} \phi_{0,g'} + Q_{0,g} \quad (5)$$

$$\frac{1}{3} \frac{d}{dx} \phi_{0,g} + \frac{2}{3} \frac{d}{dx} \phi_{2,g} + \Sigma_{1,g} \phi_{1,g} = 0 \quad (6)$$

$$\frac{2}{5} \frac{d}{dx} \phi_{1,g} + \frac{3}{5} \frac{d}{dx} \phi_{3,g} + \Sigma_{2,g} \phi_{2,g} = 0 \quad (7)$$

$$\frac{3}{7} \frac{d}{dx} \phi_{2,g} + \Sigma_{3,g} \phi_{3,g} = 0. \quad (8)$$

Defines:

$$D_{0,g} = \frac{1}{3\Sigma_{1,g}}$$

$$D_{2,g} = \frac{9}{35\Sigma_{3,g}}$$

$$\Phi_{0,g} = \phi_{0,g} + 2\phi_{2,g}$$

$$\Phi_{2,g} = \phi_{2,g}.$$

P_3 equations (3)

$$-D_{0,g} \frac{d^2}{dx^2} \Phi_{0,g} + \Sigma_{0,g} \Phi_{0,g} - 2\Sigma_{0,g} \Phi_{2,g} = S_{0,g} \quad (9)$$

$$-D_{2,g} \frac{d^2}{dx^2} \Phi_{2,g} + \left(\Sigma_{2,g} + \frac{4}{5} \Sigma_{0,g} \right) \Phi_{2,g} - \frac{2}{5} \Sigma_{0,g} \Phi_{0,g} = -\frac{2}{5} S_{0,g} \quad (10)$$

where

$$S_{0,g} = \sum_{g' \neq g}^G \Sigma_{s0,g' \rightarrow g} (\Phi_{0,g'} - 2\Phi_{2,g'}) + \frac{\chi_g}{k_{eff}} \sum_{g'=1}^G \nu \Sigma_{f,g'} (\Phi_{0,g'} - 2\Phi_{2,g'}) + Q_{0,g}.$$



SP₃ approximation

- P_N : yields the exact transport solution as $N \rightarrow \infty$.
- 3D: $(N + 1)^2$ equations.
- 1D: $(N + 1)$ equations yield $(N + 1)/2$.
- SP_N approximation replaces $\frac{d^2}{dx^2}$ by Δ .



SP₃ equations

$$-D_{0,g}\Delta\Phi_{0,g} + \Sigma_{0,g}\Phi_{0,g} - 2\Sigma_{0,g}\Phi_{2,g} = S_{0,g} \quad (11)$$

$$-D_{2,g}\Delta\Phi_{2,g} + \left(\Sigma_{2,g} + \frac{4}{5}\Sigma_{0,g}\right)\Phi_{2,g} - \frac{2}{5}\Sigma_{0,g}\Phi_{0,g} = -\frac{2}{5}S_{0,g}. \quad (12)$$

With the Marshak vacuum BCs [1]

$$\frac{1}{4}\Phi_{0,g} \pm \frac{1}{2}\hat{n} \cdot J_{0,g} - \frac{3}{16}\Phi_{2,g} = 0 \quad (13)$$

$$-\frac{3}{80}\Phi_{0,g} \pm \frac{1}{2}\hat{n} \cdot J_{2,g} + \frac{21}{80}\Phi_{2,g} = 0 \quad (14)$$

where

$$J_{n,g} = -D_{n,g}\nabla\Phi_{n,g}.$$

Weak form

Example Code

Strong Form

$$\rho C_p \frac{\partial T}{\partial t} - \nabla \cdot k(T, B) \nabla T = f$$

Weak Form

$$\int_{\Omega} \rho C_p \frac{\partial T}{\partial t} \psi_i + \int_{\Omega} k \nabla T \cdot \nabla \psi_i - \int_{\partial \Omega} k \nabla T \cdot \mathbf{n} \psi_i - \int_{\Omega} f \psi_i = 0$$

Kernel Kernel BoundaryCondition Kernel

Actual Code

```
return _k[_qp]*_grad_u[_qp]*_grad_test[_i][_qp];
```

Figure: Translation into MOOSE kernels procedure [4].



Weak form: Equation 1

$$\begin{aligned}
 & \langle D_{0,g} \nabla \Phi_{0,g}, \nabla \Psi \rangle - \langle D_{0,g} \nabla \Phi_{0,g}, \Psi \rangle_{BC} + \langle \Sigma_{0,g} \Phi_{0,g}, \Psi \rangle + \langle -2\Sigma_{0,g} \Phi_{2,g}, \Psi \rangle \\
 & + \left\langle - \sum_{\substack{g'=1 \\ g' \neq g}}^G \Sigma_{s0,g' \rightarrow g} (\Phi_{0,g'} - 2\Phi_{2,g'}), \Psi \right\rangle \\
 & + \left\langle - \frac{\chi_g}{k_{eff}} \sum_{g'=1}^G \nu \Sigma_{f,g'} (\Phi_{0,g'} - 2\Phi_{2,g'}), \Psi \right\rangle + \langle -Q_{0,g}, \Psi \rangle = 0
 \end{aligned} \tag{15}$$

with the boundary condition

$$\langle D_{0,g} \nabla \Phi_{0,g}, \Psi \rangle_{BC} = \left\langle \frac{1}{2} \Phi_{0,g} - \frac{3}{4} \Phi_{2,g}, \Psi \right\rangle_{BC}. \tag{16}$$

Weak form: Equation 2

$$\begin{aligned}
& \langle D_{2,g} \nabla \Phi_{2,g}, \nabla \Psi \rangle - \langle D_{2,g} \nabla \Phi_{2,g}, \Psi \rangle_{BC} + \left\langle \left(\Sigma_{2,g} + \frac{4}{5} \Sigma_{0,g} \right) \Phi_{2,g}, \Psi \right\rangle \\
& + \left\langle -\frac{2}{5} \Sigma_{0,g} \Phi_{0,g}, \Psi \right\rangle + \left\langle \frac{2}{5} \sum_{g' \neq g}^G \Sigma_{s0,g' \rightarrow g} (\Phi_{0,g'} - 2\Phi_{2,g'}), \Psi \right\rangle \\
& + \left\langle \frac{2}{5} \frac{\chi_g}{k_{eff}} \sum_{g'=1}^G \nu \Sigma_{f,g'} (\Phi_{0,g'} - 2\Phi_{2,g'}), \Psi \right\rangle + \left\langle \frac{2}{5} Q_{0,g}, \Psi \right\rangle = 0. \quad (17)
\end{aligned}$$

with the boundary condition

$$\langle D_{2,g} \nabla \Phi_{2,g}, \Psi \rangle_{BC} = \left\langle -\frac{3}{40} \Phi_{0,g} + \frac{21}{40} \Phi_{2,g}, \Psi \right\rangle_{BC}. \quad (18)$$

SP3 Kernels: Equation 1

Table: SP₃ kernels.

Kernel	Equation 1
P3Diffusion	$\langle D_{0,g} \nabla \Phi_{0,g}, \nabla \Psi \rangle$
P3SigmaR	$\langle \Sigma_{0,g} \Phi_{0,g}, \Psi \rangle$
P3SigmaCoupled	$\langle -2\Sigma_{0,g} \Phi_{2,g}, \Psi \rangle$
P3InScatter	$\left\langle -\sum_{g' \neq g}^G \Sigma_{s0,g' \rightarrow g} (\Phi_{0,g'} - 2\Phi_{2,g'}), \Psi \right\rangle$
P3FissionEigenKernel	$\left\langle -\frac{\chi_g}{k_{eff}} \sum_{g'=1}^G \nu \Sigma_{f,g'} (\Phi_{0,g'} - 2\Phi_{2,g'}), \Psi \right\rangle$
BodyForce	$\langle -Q_{0,g}, \Psi \rangle$
BC Kernel	
Vacuum	$\langle \frac{1}{2} \Phi_{0,g} - \frac{3}{4} \Phi_{2,g}, \Psi \rangle_{BC}$

SP3 Kernels: Equation 2

Table: SP₃ kernels.

Kernel	Equation 2
P3Diffusion	$\langle D_{2,g} \nabla \Phi_{2,g}, \nabla \Psi \rangle$
P3SigmaR	$\langle (\Sigma_{2,g} + \frac{4}{5} \Sigma_{0,g}) \Phi_{2,g}, \Psi \rangle$
P3SigmaCoupled	$\langle -\frac{2}{5} \Sigma_{0,g} \Phi_{0,g}, \Psi \rangle$
P3InScatter	$\langle \frac{2}{5} \sum_{g' \neq g}^G \Sigma_{s0,g' \rightarrow g} (\Phi_{0,g'} - 2\Phi_{2,g'}), \Psi \rangle$
P3FissionEigenKernel	$\langle \frac{2}{5} \frac{\chi_g}{k_{eff}} \sum_{g'=1}^G \nu \Sigma_{f,g'} (\Phi_{0,g'} - 2\Phi_{2,g'}), \Psi \rangle$
BodyForce	$\langle \frac{2}{5} Q_{0,g}, \Psi \rangle$
BC Kernel	
Vacuum	$\langle -\frac{3}{40} \Phi_{0,g} + \frac{21}{40} \Phi_{2,g}, \Psi \rangle_{BC}$



Moltres

$$\nabla \cdot D_g \nabla \phi_g - \Sigma_g^r \phi_g + \sum_{g' \neq g}^G \Sigma_{g' \rightarrow g}^s \phi_{g'} + \chi_g^t \sum_{g'=1}^G \frac{1}{k_{eff}} \nu \Sigma_{g'}^f \phi_{g'} + Q_g = 0. \quad (19)$$

Benchmark definition

- 7-group cross-sections: C5G7 [5].
- Capilla et al [3]: C5G2.

vacuum					
R	R	R	R	R	R
R	UO ₂	MOX	MOX	UO ₂	R
R	MOX	UO ₂	UO ₂	MOX	R
R	MOX	UO ₂	UO ₂	MOX	R
R	UO ₂	MOX	MOX	UO ₂	R
R	R	R	R	R	R
vacuum					

Figure: 2-D C5 MOX benchmark configuration. Image reproduced from [3]. *R* represents the reflectors.

Benchmark definition (2)

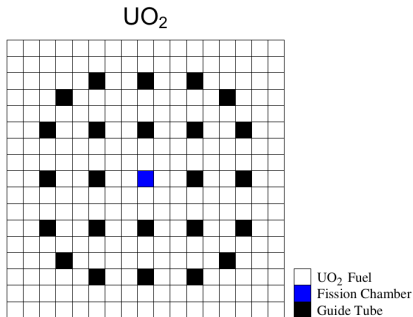


Figure: UO₂ assembly. Image reproduced from [3].

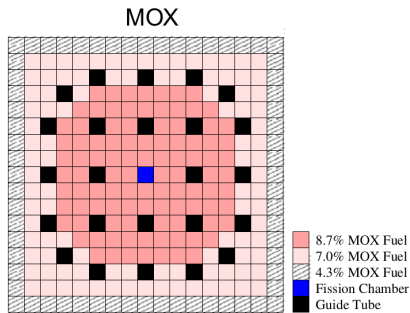


Figure: MOX assembly. Image reproduced from [3].

Benchmark geometry

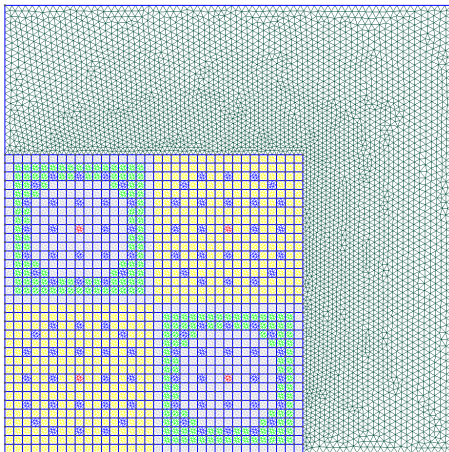


Figure: Gmsh 2D geometry.

Outline

1 Introduction

Objectives

2 Methodology

MOOSE

SP_3

Kernels

Diffusion solver

C5 MOX Benchmark

3 Results

1-D test case

2-D test case

4 Conclusions

Conclusions

Fixed source

Comparison between SP_3 and Diffusion solutions of the scalar flux.

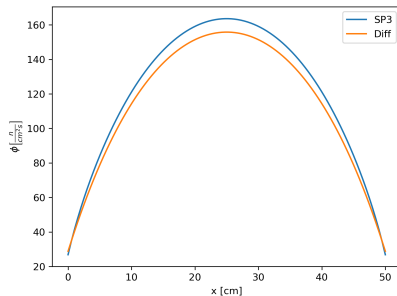


Figure: 1 group.

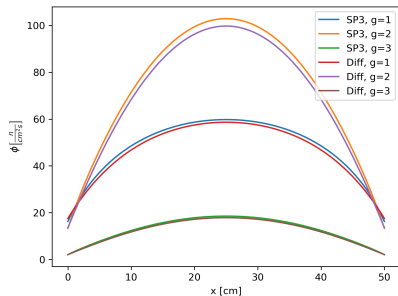


Figure: 3 groups.

Eigenvalue problem

Comparison between SP_3 and Diffusion solutions of the scalar flux. Solutions are normalized to the maximum value of the flux (fast flux for the 3 group case).

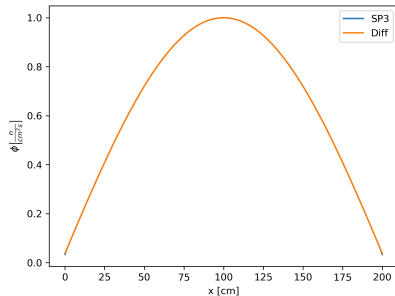


Figure: 1 group.

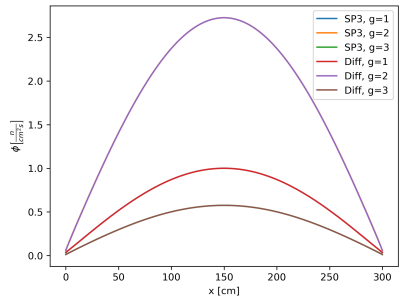


Figure: 3 groups.

C5G2 MOX Benchmark

C5G2 Benchmark		SP3	
Case	k_{Ref}	k_{SP3}	Δ_ρ [pcm]
Heterogeneous	0.96969	0.97106	145
Homogeneous	0.96983	0.97061	83

C5G2 MOX Benchmark (2)

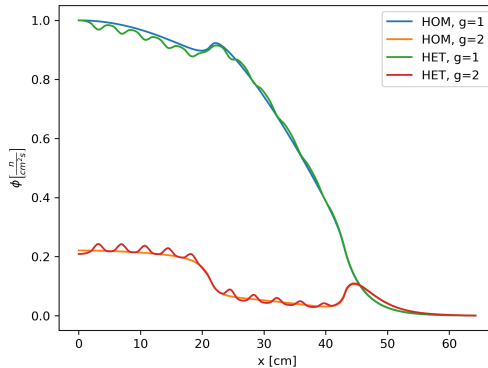


Figure: Comparison of the heterogeneous and homogeneous cases scalar flux.

C5G2 MOX Benchmark (3)

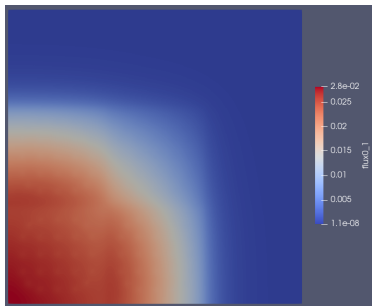


Figure: $\Phi_{0,1}$.

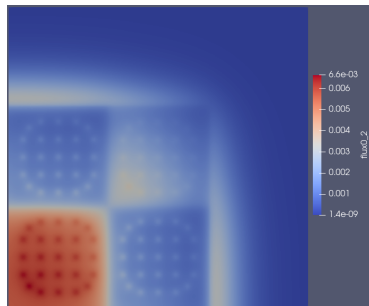


Figure: $\Phi_{0,2}$.

C5G2 MOX Benchmark (4)

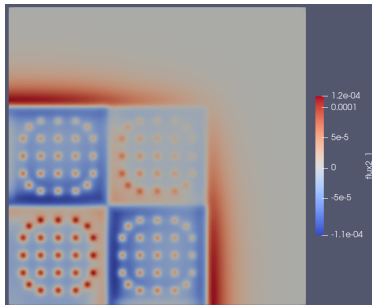


Figure: $\Phi_{2,1}$.

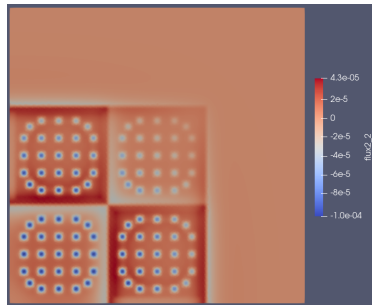


Figure: $\Phi_{2,2}$.

Outline

1 Introduction

Objectives

2 Methodology

MOOSE

SP_3

Kernels

Diffusion solver

C5 MOX Benchmark

3 Results

1-D test case

2-D test case

4 Conclusions

Conclusions



Conclusions

- 2-D test case: suggest SP_3 equations implementation is correct
- 1-D test cases: solutions are very similar to diffusion solution
- SP_N have a higher computational expense than diffusion
- further studies are necessary to conclude anything on the accuracy
- In general, SP_N are more accurate than diffusion [2]
- Less computational expense than S_N or P_N
- the study cases do not show an increased accuracy over diffusion

References I

- [1] C. Beckert and U. Grundmann.
Development and verification of a nodal approach for solving the multigroup P3 equations.
Annals of Nuclear Energy, 2007.
- [2] P.S. Brantley and E.W. Larsen.
The Simplified P3 Approximation.
Nuclear Science and Engineering, 2000.
- [3] M. Capilla, D. Ginestar, and G. Verdú.
Applications of the multidimensional equations to complex fuel assembly problems.
Annals of Nuclear Energy, 36(10):1624–1634, October 2009.
- [4] INL.
Moose Workshop Slides, December 2020.
<https://mooseframework.inl.gov/workshop>.
- [5] OECD/NEA.
Benchmark on Deterministic Transport Calculations Without Spatial Homogenisation: A 2-D/3-D MOX Fuel Assembly Benchmark.
Technical Report NEA/NSC/DOC(2003)16, OECD, 2003.